Clay Minerals, (2017) **52**, 469–483

Synthesis of nontronite and other Fe-rich smectites: a critical review

S. PETIT[1,*], F. BARON[2] AND A. DECARREAU[1]

[1] *Institut de Chimie des Milieux et Matériaux de Poitiers - IC2MP, UMR CNRS 7285, Université de Poitiers, F-86073 Poitiers Cedex 9, France*

[2] *Laboratoire de Planétologie et Géodynamique - LPG, UMR CNRS 6112, Université de Nantes, F-44300 Nantes, France*

(*Received 22 September 2017; revised 18 December 2017; Editor: G. Christidis*)

ABSTRACT: The synthesis of clay minerals has been studied for decades in an attempt to better understand their formation in natural environments and more recently to obtain clay minerals with controlled compositions and properties. Even though nontronite has been synthesized successfully since 1935, the process is not a straightforward and has been poorly documented. In the present review concerning the synthesis of nontronite and other Fe-rich smectites, the experiments attempted in the past are discussed critically in light of the most recent data. Most notably, the application of relationships established recently, thanks to synthetic smectitic series, have allowed us to refine the chemical compositions of some nontronites synthesized previously.

KEYWORDS: nontronite, iron, synthesis, hydrothermal, clay minerals, smectite, redox.

Smectites are common clay minerals occurring in various types of soils and sediments (*e.g.* Wilson, 2013). Smectites are relatively important among clay minerals because of their large specific surface areas (due to their small particles size, generally <1 μm) and ion-exchange properties. These specific physical and chemical properties make them unique and lead to a great variety of applications (Zhou, 2010).

Smectites are found the world over, but they occur only rarely as large, mono-mineralic deposits with homogeneous chemical compositions. Mineral syntheses in the laboratory have been performed to obtain clay minerals with controlled compositions and properties (see reviews by Kloprogge *et al.*, 1999; Zhang *et al.*, 2010). For smectites, most such syntheses were devoted to trioctahedral and Al-rich smectites (Kloprogge *et al.*, 1999; Zhang *et al.*, 2010). The present study is devoted exclusively to the synthesis of nontronite and other Fe-rich smectites. Natural Fe-rich smectites are generally neoformed authigenic clays occurring in various environments: weathered rocks and soils, oceanic sediments and hydrothermal deposits (see an extended review of smectite paragenesis by Wilson, 2013). The formation temperatures of these natural smectites range between 2–3°C for authigenic nontronites in deep-sea sediments and ~150°C for hydrothermal deposits (Wilson, 2013). Nontronite can also form from late-stage magmatic, granitic fluids at higher temperatures than those of hydrothermal origin (Oyawoye & Hirst, 1964). Similarly, Meunier *et al.* (2008) described post-magmatic nontronites formed when the residual liquids are concentrated in the diktytaxitic voids of basaltic rocks. The interest in Fe-smectites was recently reinforced by their widespread detection on the surface of Mars (Poulet *et al.*, 2005; Mustard *et al.*, 2008; Carter *et al.*, 2013, 2015) and generated discussion concerning their origin (Wray *et al.*, 2009; Milliken & Bish, 2010; Meunier *et al.*, 2012; Carter *et al.*, 2013; Ehlmann *et al.*, 2013; Berger

---

* E-mail: sabine.petit@univ-poitiers.fr
https://doi.org/10.1180/claymin.2017.052.4.05

et al., 2014; Mangold *et al.*, 2016). In natural Fe-rich smectites, Si, Al^{3+} and to a lesser degree Fe^{3+}, occupy tetrahedral sites, while Mg^{2+}, Fe^{2+}, Fe^{3+} and Al^{3+} commonly occupy octahedral sites. Heterovalent substitutions create a negative charge (tetrahedral charge due to R^{3+} for Si tetrahedral substitutions, and octahedral charge due to R^{2+} for R^{3+} octahedral substitutions). Due to the great variability in their chemical composition, the structural formulae of smectites range between those of dioctahedral $[^4(\mathrm{Si}_{4-x}R^{3+}{}_x)^6(R^{3+}{}_{2-y}R^{2+}{}_y)\mathrm{O}_{10}(\mathrm{OH})_2M^+{}_{x+y}]$ and trioctahedral $[^4(\mathrm{Si}_{4-x}R^{3+}{}_x)\ ^6(R^{2+}{}_{3-y}R^{3+}{}_y)\mathrm{O}_{10}(\mathrm{OH})_2M^+{}_{x-y}]$. The most common smectite end-members are montmorillonite $[^4(\mathrm{Si}_4)^6(\mathrm{Al}_{2-y}\mathrm{Mg}\text{-}R^{2+}{}_y)\mathrm{O}_{10}(\mathrm{OH})_2M^+{}_y]$, beidellite $[^4(\mathrm{Si}_{4-x}\mathrm{Al}_x)^6(\mathrm{Al}\text{-}R^{3+})_2\mathrm{O}_{10}(\mathrm{OH})_2M^+{}_x]$, nontronite $[^4(\mathrm{Si}_{4-x}(\mathrm{Al}\text{-}\mathrm{Fe}^{3+})_x\ ^6((\mathrm{Fe}^{3+}\text{-}\mathrm{Al})_{2-y}(\mathrm{Fe}^{2+}\text{-}\mathrm{Mg})_y))\mathrm{O}_{10}(\mathrm{OH})_2M^+{}_{x+y}]$, and saponite $[^4(\mathrm{Si}_{4-x}\mathrm{Al}_x)^6(\mathrm{Mg}\text{-}\mathrm{Fe}^{2+})_3\mathrm{O}_{10}(\mathrm{OH})_2M^+{}_{x+y}]$, where M^+ is an exchangeable interlayer cation and $^4(\ )$ and $^6(\ )$ refer to tetrahedral and octahedral sites, respectively (Brigatti *et al.*, 2013). Many natural Fe^{3+}-rich smectites are generally intermediate between tetrahedrally charged smectites (beidellite – nontronite series : $^4(\mathrm{Si}_{4-x}(\mathrm{Al}\text{-}\mathrm{Fe}^{3+}))^6(\mathrm{Al},\mathrm{Fe}^{3+})_2\mathrm{O}_{10}(\mathrm{OH})_2M^+{}_x$), and octahedrally charged smectites (montmorillonite and Fe^{3+}-montmorillonite series : $^4(\mathrm{Si}_4)\ ^6((\mathrm{Al}\text{-}\mathrm{Fe}^{3+})_{2-y}R^{2+}{}_y)\mathrm{O}_{10}(\mathrm{OH})_2M^+{}_y$) ($R^{2+}$ being Mg or Fe). Natural Fe^{2+}-rich smectites are generally saponites: $^4(\mathrm{Si}_{4-x}\mathrm{Al}_x)^6(R^{2+}{}_3)\mathrm{O}_{10}(\mathrm{OH})_2M^+{}_x$, ($R^{2+}$ being Mg and Fe). Numerous theoretical Fe-smectitic end-members can be thus defined, such as $^4(\mathrm{Si}_{4-x}\mathrm{Fe}^{3+}{}_x)^6(\mathrm{Al}_2)\mathrm{O}_{10}(\mathrm{OH})_2M^+{}_x$ (only theoretical, see below), $^4(\mathrm{Si}_{4-x}\mathrm{Al}_x)^6(\mathrm{Fe}^{3+}{}_2)\mathrm{O}_{10}(\mathrm{OH})_2M^+{}_x$ (nontronite), $^4(\mathrm{Si}_{4-x}\mathrm{Fe}^{3+}{}_x)\ ^6(\mathrm{Fe}^{3+}{}_2)\mathrm{O}_{10}(\mathrm{OH})_2M^+{}_x$ (ferric nontronite), $^4(\mathrm{Si}_4)^6(\mathrm{Fe}^{3+}{}_{2-x}\mathrm{Mg}_x)\mathrm{O}_{10}(\mathrm{OH})_2M^+{}_x$ (ferric montmorillonite), $^4(\mathrm{Si}_{4-x}\mathrm{Fe}^{3+}{}_x)\ ^6(\mathrm{Mg}_3)\mathrm{O}_{10}(\mathrm{OH})_2M^+{}_x$, (ferric saponite), $^4(\mathrm{Si}_{4-x}\mathrm{Al}_x)^6(\mathrm{Fe}^{2+}{}_3)\mathrm{O}_{10}(\mathrm{OH})_2M^+{}_x$ (ferrous saponite), *etc*. Numerous questions arise when establishing the structural formulae for natural Fe-rich smectites: what is the extent of substitution of the main octahedral cations Al, Fe and Mg? How are Al^{3+} and Fe^{3+} distributed between the octahedral and tetrahedral sites, and, in particular, what is the amount of tetrahedral Fe? Infrared (IR) and Mössbauer spectroscopy, among other techniques, is often used to constrain the structural formulae of natural clay minerals (*e.g.* Goodman *et al.*, 1976; Bonnin *et al.*, 1985; Cardile & Johnston, 1985; Slonimskaya *et al.*, 1986; Madejová *et al.*, 1994; Gaudin *et al.*, 2004a, 2004b; Gates, 2005; Cashion *et al.*, 2008; Kaufhold *et al.*, 2017). However, interpretation of spectroscopic features is generally not unambiguous.

Mineral synthesis in the laboratory was of interest in preparing Fe-rich smectites with unique crystal-chemistry:

(1) for better interpretation of their spectroscopic features (see Andrieux & Petit, 2010; Petit *et al.* 2015, 2016; Baron *et al.*, 2016a), for IR spectroscopy in both the mid- and near-IR regions, and, for Mössbauer spectroscopy (Baron *et al.*, 2017).

(2) to better constrain the conditions of formation of smectite, *e.g.* the synthesis temperature of nontronite was given as 340°C (Ewell & Insley, 1935), 200°C (Hamilton & Furtwängler, 1951), 90–100°C (Tomita *et al.*, 1993) and 3–20°C (Harder, 1976), revealing the wide temperature range suitable for nontronite formation. Farmer *et al.* (1991, 1994) and Farmer (1997) suggested that the widespread occurrence of ferruginous beidellites in Vertisols under Mediterranean and subtropical climates was linked to the presence of ferrous Fe, cyclic oxidizing and reducing conditions and alkaline pH (Farmer *et al.* 1991, 1994; Farmer, 1997). Thus, to understand better the formation of Fe-beidellite in Vertisols, Farmer *et al.* (1991, 1994) and Farmer (1997) performed syntheses of Al-Fe-Mg smectites at temperatures of 23–95°C.

(3) to obtain materials of interest for many applications such as in catalysis (*e.g.* Zen *et al.*, 1996; Liu *et al.*, 2014; Li *et al.*, 2015), degradation or retention of organic compounds (*e.g.* Gupta *et al.*, 2006; Hofstetter *et al.*, 2006; Neumann *et al.*, 2009), reduction of mobility of heavy metals (*e.g.* Jaisi *et al.*, 2009; Yang *et al.*, 2012; Ilgen *et al.*, 2012), liquid crystals (*e.g.* Michot *et al.*, 2008, 2009, 2013; Paineau *et al.*, 2013; MacGregor-Ramiasa *et al.*, 2015) or potentially for geological disposal of high-level nuclear waste (Nagase *et al.*, 1999).

HISTORICAL RECORD OF SYNTHESES OF Fe-RICH SMECTITES

Ewell & Insley (1935) were the first to report the synthesis of nontronite (Table 1) along with kaolinite and beidellite, to better understand the conditions of formation of natural clay minerals. The synthesis was performed from an Fe_2O_3-$2SiO_2$ starting gel obtained from solutions ($2\ \mathrm{FeCl}_3 + 2\mathrm{SiNa}_2\mathrm{O}_3 + \mathrm{NaOH}\ 10\%$). The gel was washed and aged at 340°C for 6 days. Some nontronite, identified by X-ray diffraction (XRD) camera films from powdered samples, mixed with hematite and a hydrous Fe silicate (not studied) were obtained. After removing hematite, the chemistry of the nontronite-hydrous Fe silicate (50% each) mixture, established by chemical analysis, was: $^4(\mathrm{Si}_{3.8}\mathrm{Fe}_{0.2})^6\mathrm{Fe}_2$ (ferric nontronite). The Fe hydrous silicate probably had a greater Si/Fe ratio than that of

TABLE 1 Published data (chronological order) for Fe-smectite syntheses.

Reference	Starting material	*T* (°C)	Time (days)	Synthetic products	Chemical data given by the authors	Recalculated SF
Ewell & Insley (1935)	Gel (Fe_2O_3-$2SiO_2$)	350	6	Nontronite + hematite + hydrated Fe silicate	$^4(Si_{3.8}Fe^{3+}_{0.2})\ ^6Fe^{3+}_2$	
Hamilton & Furtwängler (1951)	Gel ($4SiO_2$-Fe_2O_3-$0.25\ Na_2O$	200	1	Nontronite	$Si_4{}^6Fe_{1.78}$	$^4(Si_{3.3}\ Fe^{3+}_{0,7})\ ^6\ Fe^{3+}_2$ (a)
Caillère *et al.* (1953)	Dilute solutions Si -Fe^{3+}-Fe^{2+}-Mg	100	≈ 30	Saponite, chlorite(?)	$^4(Si_{3.6}\ Fe^{3+}_{0.4})\ ^6(Fe^{3+}_1Mg_{1.1}\ Fe^{2+}_{0.16})$	
Caillère *et al.* (1955)	Dilute solutions Si - Fe^{3+} -Al- Mg	100	≈ 30?	Nontronite	$^4(Si_{3.33}Al_{0.15}\ Fe^{3+}_{0.52})^6(Fe^{3+}_{2,06}\ M_{g0.21})$	
Kopp (1967)		365	≈ 90	Grünerite + ε aegirine + ε nontronite	?	
Harder (1976, 1978)	Gel (Fe $^{2+}$-Si)	3; 20	3 to 30	Nontronite, lembergite	$0 < {}^4Fe^{3+} < 0.5$	
Decarreau & Bonnin (1986)	Gel (Fe^{2+}-Si)	75	30 (15 reducing)	Nontronite	$Si_4{}^6Fe^{3+}_{2.95}$	$(Si_{3.83}\ ^4Fe^{3+}_{0.17})^6Fe^{3+}_2$ (a, b)
Decarreau *et al.* (1987)	Gel (Fe^{3+}-Si)	75; 100 150	30 12	Nontronite	$Si_4\ ^6Fe^{3+}_{1.83}$	$^4(Si_{3.7}Fe^{3+}_{0.3})\ ^6Fe^{3+}_2$ (b)
Mizutani *et al.* (1991)	$FeSO_4 + SiNa_2O_3 +$ NaOH (Si/Fe/OH = 1.33/1/7)	150	2	Nontronite	$^4Fe^{3+} = 44.8\%;{}^6Fe^{3+} = 51.7\%;$ $^6Fe^{2+} = 3.5\%$	$^4Fe^{3+} = 0.7$ (c) $^4Fe^{3+} = 24.2\%;{}^6Fe^{3+} = 72.2\%;\ ^6Fe^{2+} = 3.5\%$ (Fig. 3)
Farmer *et al.* (1991)	Gel (Fe^{2+}-Al-Si)	23; 89	84	Nontronite, beidellite		$^4(Si\ _{3.27}Fe^{3+}_{0.73})^6Fe^{3+}_2$ (1)
Tomita *et al.* (1993)	Volcanic glass + NaOH	90	3; 7	Al-Fe-Mg smectite	$^4(Si_{3.75}Al_{0.9}Ti_{0.18})\ ^6(Mg_{0.48}Fe^{3+}_{0.65}Al_{0.9})$	
Farmer *et al.* (1994)	Gel (Fe^{2+}-Al-Si)+ $Ca(OH)_2$ or KOH	70; 92	18 to 56	Al-nontronite	$^4(Si_{3.33}Al_{0.67})\ ^6(Al_{0.6}Fe_{1.4})$(2)	$^6(Al\ _{0.83}\ Fe\ _{1.17})$ (a)
Grauby *et al.* (1994)	Gel (Si-Fe^{3+}-Mg)	200		Nontronite Fe^{3+}-Mg	$^4(Si_{4-x}Fe^{3+}{}_x)\ ^6(Fe^{3+}{}_yMg_z)$ $x = 0$ to 0.17; $y = 0.3$ to 1.88; $z = 0.08$ to 2.43	
Farmer (1997)	Gel (Fe^{2+}-Al-Si)	95	70 to 91	Al-Fe beidellites	$^4(Si_{3.41}Al_{0.59})\ ^6(Al_{1.18}Fe_{0.82})$ (3)	$^6Fe = 0.8$ (4); $^6Fe = 2.6$ (5) (a, b)

(continued)

TABLE 1 (*contd.*)

Reference	Starting material	T (°C)	Time (days)	Synthetic products	Chemical data given by the authors	Recalculated SF
Lajarige *et al.* (1998)	Gels (Fe $^{2+}$-Al- Mg-Si)	200	41	Al-Fe-Mg smectite	$^4(Si_{3.74}Al_{0.26})\ ^6(Al_{1.06}\ Fe^{3+}_{0.8}Fe^{2+}_{0.2})$ $^4(Si_{3.7}Al_{0.3})^6(Al_1Fe^{3+}_{0.97}Fe^{2+}_{0.03})$	
Nagase *et al.* (1999)	Gel (Si-Fe^{3+}-Mg)	100; 200	24	Fe^{3+}- Mg smectite	Si/Fe/Mg = 4/1.65/0.3	$0 < {}^4Fe < 0.5$ (a)
Decarreau *et al.* (2004)	Gel (Fe $^{2+}$-Si)	200	28	Aegirine + ε nontronite	$^4(Si_{4-x}Fe^{3+}{}_x)\ ^6Fe^{3+}_2(x = ?)$	$^4Fe = 0.31$ (b)
Decarreau *et al.* (2008)	Gel (Fe $^{2+}$-Si)	75;90;100; 110;125;150	28	Nontronites	$^4(Si_{3.25}Fe^{3+}_{0.75})\ ^6Fe^{3+}_2$	
Andrieux & Petit (2010)	Gel (Fe^{2+}-Al-Si)	150–240	13 to 75	Al-Fe^{3+} nontronites	$^4(Si_{4-x}(Fe^{3+}, Al)_x)^6(Fe^{3+}_{2-y}Al\ _y)$ $x = 0.3$ to 0.75; $y = 0$ to 1.88	
Baldermann *et al.* (2014)	Gel (Si-Fe^{2+}-Mg)	120, 180	2, 5, 7	(Fe^{2+}-Fe^{3+}-Mg) saponites	$^4(Si_{4-x}Fe^{3+}{}_x)\ ^6(Fe^{2+}{}_z,Fe^{3+}{}_y,\ Mg_w)$ $x = 0.06–0.26$; $z = 0.42–2.28$; $y = 0.03–0.23$; $w = 0.26–2.78$	
Petit *et al.* (2016)	Gels (Fe^{3+}-Ga-Si)	180	18	Ga-Fe^{3+} nontronites	$^4(Si_{4-x}(Fe^{3+},Ga)_x\ ^6(Fe^{3+}_{2-y}Ga_y)$ $x = 0.45$ to 0.75; $y = 0$ to 2	
Baron *et al.* (2016a)	Gel (Fe^{2+}-Si)	150	6	Nontronites	$^4(Si_{4-x}Fe^{3+}{}_x)\ ^6Fe^{3+}_2$ $x = 0.43$ to 1.54	

Chemical data for synthesized nontronites are given per $O_{10}(OH)_2$. ε: identified in trace; SF: structural formula. The SF were partially recalculated using established relationships (Table 2) when possible from: (a) XRD $d_{06,33}$ values; (b) IR spectra; (c) Mössbauer spectra. Numbers in parentheses refer to the Si/Al/Fe/Mg ratio of the starting gels used by Farmer *et al.* (1991, 1994) and Famer (1997) (1): 6/0/4/0; (2): 6/2/2/0; (3): 15/5/2/0; (4) 14/5/5/0; (5): 15/5/2/0.

nontronite. The same ageing from a mixture of Fe_2O_3 and SiO_2 gels yielded hematite and cristobalite instead of nontronite.

Hamilton & Furtwängler (1951) used a starting gel with a $SiO_2/Fe_2O_3/Na_2O$ ratio of 4/1/0.25. 0.25 g of gel was aged for 24 h at temperatures between 175 and 350°C, in 3 cm^3 of water. The most favourable temperature was 200°C. The structural formula of the ferric nontronite synthesized, determined using XRD, differential thermal analysis (DTA) and chemical analyses, was $Si_4Fe_{1.78}O_{10}(OH)_2Na_{0.33}$, not balanced but clearly in accordance with the chemical composition of ferric nontronite. Caillère *et al.* (1953, 1955) performed syntheses of Fe-rich smectites by adding droplets (one drop per 20 s) of diluted solutions of Si $(OH)_4$ (<10 mg L^{-1}), Mg, Fe^{2+}, and Fe^{3+} chlorides (10–50 mg L^{-1}) to boiling water at pH fixed between 8.5 and 9.5 by addition of small quantities of acid or base. After ~1 month, 25–125 mg of solids was obtained. From XRD, DTA and chemical analyses, the synthesized smectites were classified as "saponites" by the authors, and had ~0.4–0.6 tetrahedral Fe^{3+}, with the octahedral sheet containing 1.0 Fe^{3+}, 1.1 Mg and 0.16 Fe^{2+} atoms per half unit cell (phuc). Syntheses performed at pH = 7–7.5 produced expanding chlorites. When Al was added, synthesis performed at pH = 8–9 produced a smectite with the following composition: $^4(Si_{3.33}Al_{0.15}Fe^{3+}_{0.52})^6(Fe^{3+}_{2.06}Mg_{0.21})$, with some Mg possibly being exchangeable.

Koop & Harris (1967) obtained nontronite and aegirine (a Na-clinopyroxene, $NaFeSi_2O_6$) as by products when studying the synthesis of grunerite (Fe^{2+}-amphibole). Syntheses were performed for 82–92 days in a furnace inducing a thermal gradient into the autoclave (425–400°C at the base; 395–365°C at the top), the pressure being 1.6 kbar and the pO_2 greater than that of the magnetite-quartz-fayalite buffer. Silica came from chips of quartz and iron from the autoclave liner, the solution being 0.1 N NaOH. Aegirine and nontronite were identified using XRD, at the base and at the top of the autoclave, respectively.

Harder (1976, 1978) studied the synthesis of Fe^{3+}-clay minerals from ferrous amorphous gels. Very dilute solutions of monomeric silica (near 20 ppm SiO_2) and $FeSO_4$ (0.3–20 ppm Fe) and sometimes Al (0.3–2 ppm Al) and/or Mg (300–1200 ppm Mg) were used. Reducing conditions were obtained by the addition of 0.03, 0.1 and 0.3% of Na-dithionate. Amorphous starting hydroxide-silica precipitates were obtained by an increase in the pH of starting solutions, or by a change in Eh. Syntheses were performed at 3–20°C for 3–30 days. The pH was fixed between 8 and 8.5 by NaOH. Successful syntheses of Fe clays were obtained for reducing conditions only. Trioctahedral TO clays were synthesized from starting solutions having a low Si/Fe ratio, while poorly crystallized TOT clays were obtained for high Si/Fe ratios. Nontronite (mainly dioctahedral Fe^{3+} smectite) and lembergite (mainly trioctahedral Fe^{2+} smectite) were identified on the basis of the $d_{\overline{06}33}$ XRD values. Chemical analyses suggested that the synthetic products were not monomineralic. Harder (1978) then concluded that the synthesis of Fe^{3+}-nontronite was possible only if: Fe^{2+} cations were present in solutions, there was a high pH and $Eh < 0$, inducing better crystallinity of these smectites.

Decarreau & Bonnin (1986) synthesized at 75°C, a ferric nontronite from a ferrous starting gel, $Si_4Fe^{2+}_3O_{11}\cdot nH_2O$, with stoichiometry corresponding to trioctahedral ferrous smectite, obtained by mixing $FeSO_4$ and SiO_2Na_2O solutions. The starting gel was first aged for 15 days under reducing conditions by bubbling hydrogen gas in the synthesis vessel. Only a very poorly crystallized ferrous stevensite was identified by XRD. After 15 days of spontaneous oxidation in contact with air, a strictly ferric nontronite was synthesized as was confirmed by Mössbauer spectroscopy. The chemical analyses corresponded to the following structural formula: $Si_4Fe^{3+}_{2.95}O_{10}(OH)_2Na_{0.05}$. This structural formula is probably invalid due to the amount of Fe^{3+} which is too great. Accordingly, from Mössbauer spectroscopy at 4 K, at the end of the synthesis, one third of Fe was located in an amorphous Fe oxide (or oxyhydroxide) phase. This amorphous Fe oxide was linked intimately to nontronite layers and was issued from the oxidation reaction of the ferrous stevensite: $[Fe^{2+}_3\text{-stevensite}] \rightarrow [Fe^{3+}_2\text{-nontronite}] + ½\, Fe_2O_3$.

The synthesis of a ferric nontronite under oxidizing conditions was managed by Decarreau *et al.* (1987) using a ferric starting gel with stoichiometry corresponding to a dioctahedral smectite: $^4(Si_4)^6(Fe^{3+}_2)O_{11}$. This gel was obtained from sodium-silicate and ferric sulfate solutions. Syntheses were performed for 1 month at 75 and 100°C and for 12 days at 150°C. The XRD and X-ray absorption fine structure (EXAFS) data showed that the synthetic product obtained at 75°C looked like germs with dioctahedral TOT structure. At 100 and 150°C, ferric nontronites were obtained. The structural formula, determined from chemical analyses of the synthetic product, was $^4(Si_4)^6(Fe^{3+}_{1.83})O_{10}(OH)_2Ca_{0.26}$. This structural formula probably does not actually correspond to the nontronite synthesized, and the presence of an excess of silica was suggested. From the increase in the crystallinity of nontronites *vs.* the synthesis temperature, the time necessary to obtain nontronite was evaluated to be of the order of 10 y at 25°C and 200 y at 2°C.

Mizutani *et al.* (1991) synthesized Fe nontronites from suspensions obtained by adding to a $SiNa_2O_3$-$FeSO_4$ solution (Fe/Si = 0.75 and 1.5), a NaOH 5 M solution and 10 g L^{-1} of Na-dithionite. Syntheses were performed at 150 and 200°C for 50 h. At 150°C, and with a Si/Fe ratio of 0.75, the nontronite obtained was pure and well crystallized, but still contained 3.5% of Fe^{2+} detected by Mössbauer spectroscopy.

Tomita *et al.* (1993) showed that smectites may form by reaction of volcanic glass with NaOH, under 1 atm. pressure at 90–100°C. Experiments were carried out for 3–10 days, using various glass/NaOH ratios. An Fe-Al-Mg beidellite (Fe/Al = 0.7, Mg/Al = 0.5) was synthesized for a low glass/NaOH ratio, while zeolites or zeolite-smectite mixtures were formed in other cases. The beidellite synthesized was not well crystallized, regardless of the time of the experiments. A *b* crystallographic parameter of 9.2 Å was measured from dotted electron diffraction patterns, suggesting an ordered stacking of beidellite layers.

Farmer *et al.* (1991, 1994) performed experiments from 23 to 95°C for 4–13 weeks. The pH was near 8–8.5 using a $Ca(OH)_2$-$CaCO_3$ buffer. The starting materials were obtained mixing various amounts of Si $(OH)_4$, $AlCl_3$, $FeCl_2$ and ($MgCl_2$ + KCl) solutions. Initial reducing conditions were obtained by addition of hydrazine, and oxidation occurred during syntheses by air diffusion. For syntheses performed at 23°C, Mg-free allophanes were identified by XRD and IR data. At 89°C allophane formed from the (Fe-Mg)-free starting product. Smectites were obtained from the initial products having Fe/Al ratios >1 and when the amount of Si in solution was >280 µmole L^{-1}. The synthesized smectite particles containing Mg, obtained in Ca + K solutions, exhibited randomly stacked layers. For the experiments without Mg, Al-Fe smectites were synthesized with layer stacking which depended on the cations occurring in solution: ordered for Ca and random for Na or K. Farmer (1997) carried out similar syntheses, without Mg, but using successive redox cycles for 10–13 weeks: reduction by adding large amounts of hydrazine, followed by oxidation for ~15 days due to air diffusion. Initial precipitates resembled allophanes and no smectite was synthesized for starting materials with Al/Fe > 3.5. Smectites with a constant chemistry were synthesized for 2.5 < Al/Fe < 3.5; the chemical analyses suggested excess Al and Fe, said to be in the interlayer space. For a starting material with a Si/Al/Fe ratio of 15/5/2, the smectite synthesized had the following structural formula: $^4(Si_{3.41}Al_{0.59})^6(Al_{1.18}Fe_{0.82})O_{10}(OH)_2Ca_{0.295}$. Farmer *et al.* (1994) concluded that the main crystallization process of synthetic Al/Fe smectites occurred during or after Fe oxidation.

Grauby *et al.* (1994) studied the heterovalent octahedral Fe^{3+}/Mg substitution *via* the hydrothermal synthesis at 200°C of a smectite series from starting gels having the $^4(Si_4)^6(Fe^{3+}_{(2-2x/3)}Mg_x)O_{11}$ theoretical stoichiometry, with x varying from 0 to 3. The starting gels were obtained from sodium metasilicate and Mg and Fe^{3+} chlorides. After combining XRD, IR, Mössbauer and transmission/analytical electron microscopy (TEM-AEM) data, those authors showed that the Fe-smectites synthesized had a small tetrahedral charge increasing from 0 to 0.17 e/huc when $^6Fe^{3+}$ increased from 0.3 to 1.88 while the ^6Mg increased from 0.08 to 2.43 (for $O_{10}(OH)_2$). The *b* crystallographic parameter was correlated linearly to the amounts of ^6Mg or ^6Fe, following Vegard's law (Table 2). The simultaneous occurrence in IR spectra of bands due to 3Mg-OH, $Mg^{2+}Fe^{3+}$-OH and $2Fe^{3+}$-OH stretching vibrations proved the segregation of ^6Mg and $^6Fe^{3+}$ cations in trioctahedral and dioctahedral local environments, respectively, within each smectite layer.

Using the procedure of Decarreau & Bonnin (1986), *i.e.* preparing the starting material under anaerobic conditions and oxidation occurring during synthesis by air diffusion into the reactors, Lajarige *et al.* (1998) synthesized Al-Fe beidellites in which some Fe remained as Fe^{2+}. Those authors performed two syntheses at 200°C for 41 days using the same starting gel with the following stoichiometry: $Si_4Al_{1.33}FeO_{11}$. According to XRD, IR and Mössbauer data, two different Al-Fe beidellites were obtained: $^4(Si_{3.7}Al_{0.3})^6(Al_1Fe^{3+}_{0.97}Fe^{2+}_{0.03})O_{10}(OH)_2Na_{0.33}$ and $^4(Si_{3.74}Al_{0.26})^6(Al_{1.06}Fe^{3+}_{0.8}Fe^{2+}_{0.2})O_{10}(OH)_2Na_{0.33}$.

Nagase *et al.* (1999) synthesized Fe-smectites at 100 and 200°C for 24 h from hydrous oxides obtained by mixing acidic sodium silicate, $FeCl_3$ and $MgCl_2$ solutions, precipitated at pH = 9.9 (pH adjusted using NaOH). Smectites were identified by XRD for a narrow pH range only between 12.0 and 12.4. When the pH was <12, an amorphous phase was detected and when the pH was >13 a mixture of aegirine and hematite was produced. From TEM-energy dispersive X-ray spectroscopy (EDS) data, the Si/Fe/Mg ratio of clay particles was 4/1.65/0.3.

Decarreau *et al.* (2008) synthesized hydrothermally (75–150°C, 4 weeks) high-charge ferric nontronite, and characterized accurately for the first time the ferric end-member of nontronite using XRD, IR, Mössbauer

TABLE 2 Correlations between the IR band position (cm^{-1}) and the (*b*) crystallographic parameter (Å) (from the $d_{06,33}$ XRD reflection) and ^{4}Fe $^{3+}$ and ^{6}Fe^{3+} amounts per O_{10} $(OH)_2$ for synthetic Fe-rich smectites.

FTIR data	XRD data
$^4Fe^{3+}$ for Al-nontronites (Petit *et al.*, 2015) ν (Si-O) = 1019 cm^{-1}–3.2 * $^4Fe^{3+}$ for Fe^{3+}-nontronites (Baron *et al.*, 2016a) ν (Si–O) = 1037 cm^{-1}–54.5 * $^4Fe^{3+}$)	$^4Fe^{3+}$ for Al-nontronites (Petit *et al.*, 2015) *b* = 9.164 Å + 0.114 * $^4Fe^{3+}$ for Fe^{3+}-nontronites (Baron *et al.*, 2016a) *b* = 9.127 Å+0.1086 * $^4Fe^{3+}$
$^6Fe^{3+}$ for Al-nontronites (Petit *et al.*, 2015) ν (Si–O) = 1040 cm^{-1}–9.56 * $^6Fe^{3+}$ $(Si–O–M)_1$ = 539 cm^{-1}–24.7 * $^6Fe^{3+}$ $(Si–O–M)_2$ = 476 cm^{-1}–12.1 * $^6Fe^{3+}$ M–O = 713 cm^{-1}–18.3 * $^6Fe^{3+}$	$^6Fe^{3+}$ for Al-nontronites (Petit *et al.*, 2015) *b* = 8.940 Å + 0.114 * $^6Fe^{3+}$
	Total Fe^{3+} for Al-nontronites (Petit *et al.*, 2015) *b* = 8.944 Å + 0.111 * Fe_{tot}
	Total Al for Al-nontronites (Petit *et al.*, 2015) *b* = 9.232 Å – 0.111 *Al_{tot}
	^{6}Al for Al-nontronites (Petit *et al.*, 2015) *b* = 9.170 Å – 0.110 * ^{6}Al
	^{6}Mg for Mg-nontronites (Grauby *et al.*, 1994) *b* = 9.087 Å + 0.028 * Mg

and X-ray absorption near-edge spectroscopy (XANES) data. The synthesis was performed from a silico-ferrous starting gel, $Si_2FeNa_2O_6.nH_2O$, produced by mixing sodium metasilicate and ferrous chloride solutions. The pH was adjusted to 12.5 by NaOH. Regardless of the synthesis temperature, the nontronite synthesized had the same structural formula: $^4(Si_{3.25}Fe^{3+}_{0.75})^6Fe^{3+}_2O_{10}(OH)_2Na^+_{075}$. The crystallinity of these nontronites increased with synthesis temperature, and their expandability moved from smectite to vermiculite-like behaviour. Aegirine, mixed with a poorly crystallized ferric nontronite, was synthesized at 200°C using the same starting gel at pH from 10 to 12 (Decarreau *et al.*, 2004).

Andrieux & Petit (2010) were the first to synthesize Al-Fe^{3+} smectites within a wide compositional range, without Mg, following the $^4(Si_{4-x}(Fe^{3+}\text{-}Al)_x)^6(Fe^{3+}_{2-y}Al_y)O_{10}(OH)_2Na_x$ structural formula. These Al-Fe^{3+} smectites were characterized carefully by coupling XRD, IR and TEM-EDS data (Petit *et al.*, 2015). The tetrahedral charge (x) ranged from 0.3 to 0.5 e/huc (0.75 for the ferric end-member) and occurred essentially by means of Al-for-Si substitutions, with tetrahedral Fe^{3+} being ~0.1 for most of the Fe-rich Al-Fe^{3+} smectites. The octahedral Al (y) ranged from 0 to 1.88. The windows of experimental conditions to crystallize such smectites are narrow. Temperatures up to 150°C and high pH (~12) are suitable for the formation of the Fe^{3+}-rich smectites (nontronite), while higher temperatures (200°C) and lower pH (down to 7) are suitable for the most Al-rich smectites (Fe^{3+}-beidellites). For intermediate compositions, both the pH and temperature of synthesis should be adjusted in parallel to favour crystallization of pure smectite. Outside these windows, admixtures or other phases were obtained.

Baldermann *et al.* (2014) synthesized Mg-Fe^{2+} saponites under reducing conditions (0.05 mass% of Na dithionite) at 120 and 180°C, over periods of 2, 5 and 7 days, the final pH being near 12.6. Initial precipitates were obtained from solutions of Na orthosilicate (Na_4SiO_4), Fe (II) sulfate ($FeSO_4 \cdot 6H_2O$) and Mg chloride salts ($MgCl_2 \cdot 6H_2O$) with molar Si: Fe:Mg ratios of 4:0:2, 4:1:1, 4:1.5:0.5, 4:1.75:0.25, and 4:1.82:0.18. The initial pH was adjusted to 8.5 with NaOH. The smectites synthesized were characterized by XRD, FTIR and TEM-EDS. The Fe^{2+}/Fe^{3+} ratios of clay particles were measured using electron energy-loss spectroscopy (EELS). The saponites synthesized were more or less mixed with by products (antigorite, nontronite, brucite, ferrihydrite, opal CT). The tetrahedral charge of the saponites synthesized, arising from Si for Fe^{3+} substitutions, was between 0.03 and 0.26 electrons (for $O_{10}(OH)_2$), and the octahedral sheet always contained Mg, Fe^{2+} and Fe^{3+} cations, the $^6(Fe^{2+}/Fe^{3+})$ ratio being ~10. Baldermann *et al.* (2014) suggested that a complete octahedral substitution may exist in ferrous saponites between Mg and ($Fe^{2+} + Fe^{3+}$) cations. Surprisingly, IR spectra of the synthesized saponites exhibited mainly dioctahedral Fe^{3+}-OH-Fe^{3+} features, probably due to possible oxidation of the samples.

Petit *et al.* (2016) synthesized a series of Fe^{3+}-Ga^{3+} smectites in order to study the IR spectral features of these smectites. Syntheses were performed at 180°C for 18 days from starting gels using Fe^{3+} and Ga nitrates and Na metasilicate. Six smectites were synthesized with intermediate chemistries ranging from the Ga to the Fe end-members. The layer charge, due to Si-Ga substitution only, decreased from 0.76 to 0.52 electrons per $O_{10}(OH)_2$ when the amount of octahedral Fe^{3+} increased. Tetrahedral Fe^{3+} occurred for the nontronite ferric end-member only, and was 0.45 electrons per $O_{10}(OH)_2$.

Studying the improvement in the process of Decarreau *et al.* (2008), Baron (2016) successfully synthesized nontronites from starting gels prepared using $FeCl_2$, $FeSO_4$, or $FeCl_3$ salts. The size of the nontronite particles was more homogeneous when hydrated gels rather than dehydrated powders were used as the starting materials (Fig. 1). Baron (2016) also synthesized hydrothermally nontronite using a microwave furnace. For conditions of 150°C over 6 days, no difference in the yield or in the crystal chemistry of the nontronites synthesized could be detected between microwave and classical furnace experiments as observed by Baron *et al.* (2016b) for trioctahedral Ni-Mg 1:1 (nepouite–lizardite) or 2:1 (pimelite–kerolite) synthetic series (220°C – 2 days). The microwave hydrothermal synthesis method is of more interest though, because it is easier to increase the reactor capacity and maintain uniform heating.

Baron *et al.* (2016a) were able to synthesize at 150°C a chemical series of strictly ferric nontronites with various tetrahedral charges across a range of initial aqueous pH values between 11 and 14 obtained by addition of NaOH. This series was characterized accurately using XRD, IR and TEM-EDS analyses.

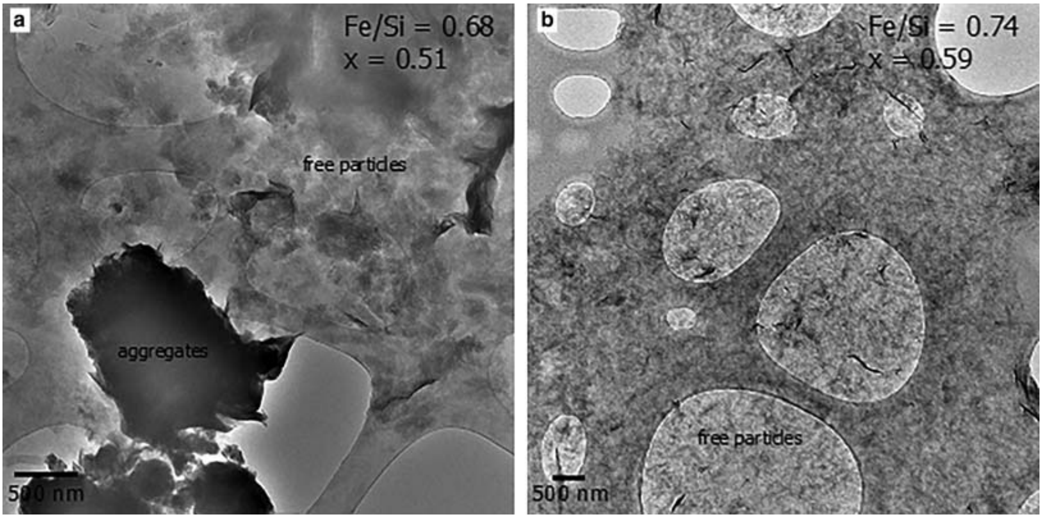

FIG. 1. TEM images of nontronites synthesized hydrothermally (6 days, 150°C) from: (a) a dehydrated powdered gel; and (b) a hydrated gel. The Fe/Si ratio was measured using SEM-EDX analyses. x was determined using the position of the νSi-O vibration and the relation developed by Baron *et al.* (2016a).

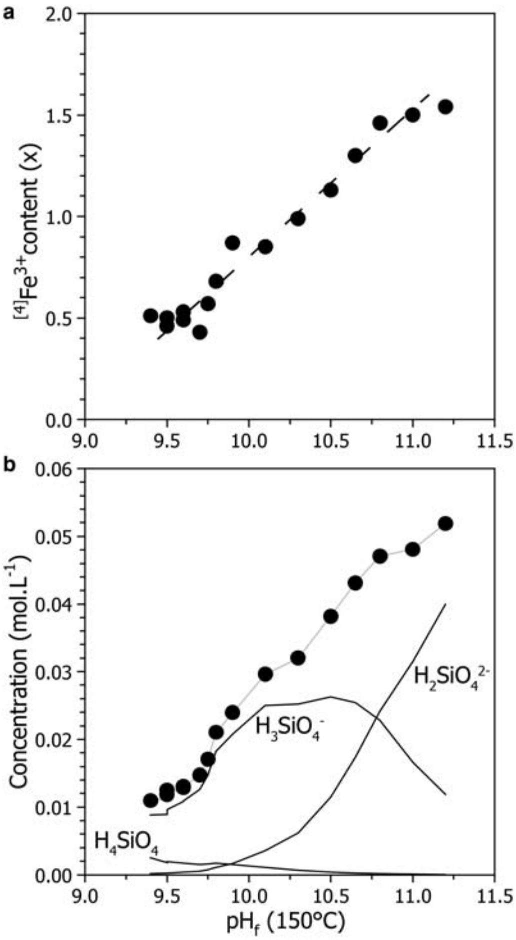

FIG. 2. Evolution, with the end-of-synthesis pH (calculated at 150°C) of: (a) the amounts of tetrahedral Fe^{3+} in the nontronites synthesized (per $O_{10}(OH)_2$); (b) the speciation and the total aqueous concentration of Si.

The permanent layer charge of synthetic nontronites, due to Fe^{3+}-for-Si tetrahedral substitutions only, ranged from 0.43 to as high as 1.54 per $O_{10}(OH)_2$. Despite the unusual values of the layer charge, synthetic Ca-saturated nontronite layers showed expansion after ethylene glycol solvation. The increase in tetrahedral Fe^{3+} was correlated with the increase in the end-of-synthesis pH measured at 25°C (Baron *et al.*, 2016a). The same trend was observed with the data recalculated for 150°C (Fig. 2). High pH values induced a strong increase in SiO_2 in solution *via* anionic aqueous Si species ratios (*i.e.* $H_3SiO_4^-$(aq) and $H_2SiO_4^{2-}$(aq)), favouring the incorporation of Fe^{3+} in the tetrahedral sites of synthetic nontronites.

QUANTIFICATION OF OCTAHEDRAL AND TETRAHEDRAL Al-Fe^{3+} CONTENTS

Thanks to recent syntheses of ferric nontronites and Al-Fe^{3+} and Ga-Fe^{3+} smectites, chemical series of Fe-rich smectites exhibiting large and continuous chemical variations were available (Andrieux & Petit, 2010; Baron *et al.*, 2016a; Petit *et al.*, 2016). Careful characterization of these synthetic smectites allowed us to establish robust correlations between XRD and IR data, and crystal-chemistry (Table 2). Petit *et al.* (2015) and Baron *et al.* (2016a) showed that the *b* lattice parameters measured by XRD, and the positions of FTIR bands, are linearly correlated with the amounts of octahedral and tetrahedral Al and Fe in the synthetic smectite (Table 2). In light of these relations, when XRD and/or spectroscopic data are available in the literature, the structural formulae for all synthetic Fe-rich smectite can be determined (or reconsidered). As an example, for the Decarreau & Bonnin (1986) ferric nontronites obtained in partly reducing conditions, both the XRD and IR independent data are consistent and led to small values for tetrahedral Fe^{3+} (0.13 and 0.17 atoms per O_{10} $(OH)_2$, respectively) (Table 1). Decarreau *et al.* (1986) were aware that the layer charge of the synthetic nontronites was particularly low, but they hypothesized that it was due to the occurrence of empty octahedral sites.

Farmer *et al.* (1991) synthesized smectites from starting gels with various Si/Al/Fe/Mg ratios. Using the available IR data and the relationships determined from chemical series (Table 2), the amounts of $^4Fe^{3+}$ and/or $^6Fe^{3+}$ in the synthetic smectites (for which no structural formulae were given) could be determined. For the 6/2/2/0 and 6/2/4/0 gels, the $^6Fe^{3+}$ value was between 1.2 and 1.5 atoms (per $O_{10}(OH)_2$) and for the 6/0/4/0 gel, the $^4Fe^{3+}$ value was 0.73, remarkably close to the 0.75 of the nontronite synthesized by Decarreau *et al.* (2008) under similar conditions.

Using the synthetic nontronite series with various tetrahedral charges described above (Baron *et al.*, 2016a), Baron *et al.* (2017) refined Mössbauer parameters (isomer shifts (δ) and quadrupoles splitting (Δ)) for tetrahedral and octahedral Fe^{3+} at ambient temperature and 77 K, using the ratio of the four possible local tetrahedral cationic environments around an octahedral Fe^{3+} (*i.e.* 4Si, 3Si-Fe^{3+}, 2Si-2Fe^{3+}). The Mössbauer spectra at ambient temperature and 95 K of a synthetic ferric nontronite given by Mizutani *et al.* (1991) were decomposed using the Baron *et al.* (2017) method (Fig. 3). A $^4Fe^{3+}$ value of 0.7 atoms (per O_{10}

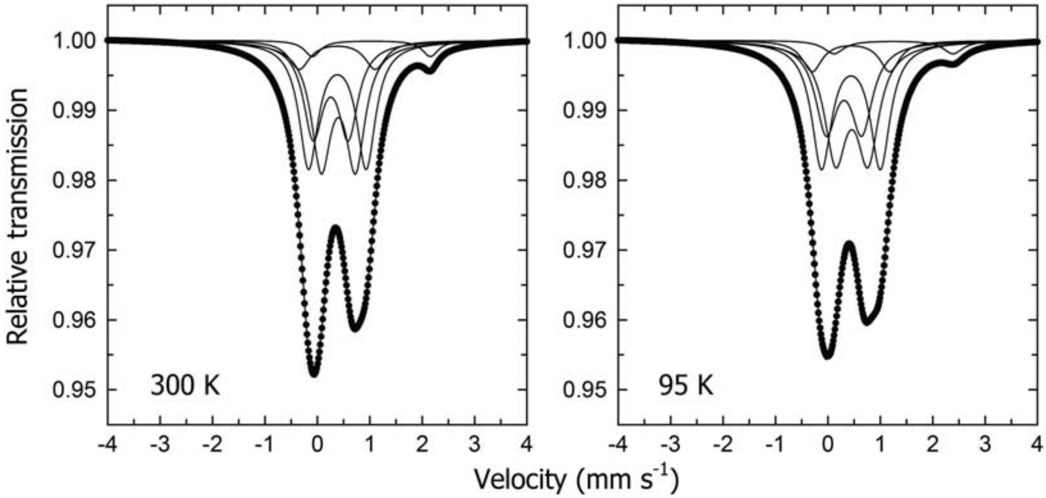

FIG. 3. Mössbauer spectra, at ambient temperature and 95 K, of a nontronite synthesized by Mizutani *et al.* (1991). The spectra were reconstructed by summation of doublets which originated using parameters found in Mizutani *et al.* (1991). The decomposition was achieved using the method of Baron *et al.* (2017) and the percentages of $^4\mathrm{Fe}^{3+}$, $^6\mathrm{Fe}^{3+}$ and $^6\mathrm{Fe}^{2+}$ determined were 24.2, 72.2 and 3.5, respectively, corresponding to an $^4\mathrm{Fe}^{3+}$ calculated value of 0.7 (per $\mathrm{O}_{10}(\mathrm{OH})_2$) (Table 2).

(OH)$_2$) was found. This value appears consistent with the synthesis conditions and all of the available data described by Mizutani *et al.* (1991).

NONTRONITE END-MEMBERS

Smectite end-members are rarely found in nature and this is the case for ferric nontronite and Al-beidellite end-members $^4(\mathrm{Si}_{4-x}\mathrm{R}^{3+}_x)^6(R^{3+})_2\mathrm{O}_{10}(\mathrm{OH})_2M^+_x$, R^{3+} being exclusively Fe or Al, respectively. The Al-beidellite end-member has been synthesized many times in the past (*e.g.* Kloprogge *et al.*, 1999; Zhang *et al.*, 2010), but always with a rather small tetrahedral charge value (x) and without focus on the tailoring of the charge. The ferric nontronite end-member was synthesized with a wide range of tetrahedral charges (x) per $\mathrm{O}_{10}(\mathrm{OH})_2$: $x = 0.2$–0.3 in Ewell & Insley (1935) and Decarreau *et al.* (1986, 1987); $x = 0.7$ in Hamilton & Furtwängler (1951), Farmer *et al.* (1991), Mizutani *et al.* (1991) and Decarreau *et al.* (2008), and x varying from 0.43 to 1.54 in Baron *et al.* (2016a). The latter authors demonstrated that the amount of $^4\mathrm{Fe}^{3+}$ in synthetic nontronites is pH dependent. The various tetrahedral charges for synthetic nontronites reported in the literature, when the values are robust, are probably due to the pH conditions of the synthesis.

The Fe^{3+} substitutes easily for Si in tetrahedral sites when it is the only M^{3+} cation used for synthesis (Table 1). When competition exists between Al and Fe^{3+}, Al occurs predominantly in tetrahedral sites and Fe^{3+} appears only when the Fe^{3+}/Al ratio is very high (Table 1). Indeed, Decarreau & Petit (2014) showed that the distribution of Al^{3+} and Fe^{3+} between octahedral and tetrahedral sites of dioctahedral smectites is controlled by a partition coefficient, $\mathrm{K_d}$:

$$\mathrm{K_d}(4/6) = [{}^4(\mathrm{Fe}^{3+}) * {}^6(\mathrm{Al}^{3+})]/[{}^6(\mathrm{Fe}^{3+}) * {}^4(\mathrm{Al}^{3+})]$$

which had a very small value (<0.02) for smectites synthesized at 200°C. Consequently, the nontronite end-member $^4(\mathrm{Si}_{4-x}\mathrm{Al}_x)^6(\mathrm{Fe}^{3+})_2\mathrm{O}_{10}(\mathrm{OH})_2M^+_x$ is theoretical because some tetrahedral Fe necessarily exists for this Fe-rich smectite, although $^4\mathrm{Fe}^{3+}$ would be very difficult to detect for $\mathrm{Fe}^{3+}/(\mathrm{Fe}^{3+}+\mathrm{Al})$ ratios of <0.6 (Decarreau & Petit, 2014). For the same reason the $^4\mathrm{Fe}^{3+}$-beidellite end-member $^4(\mathrm{Si}_{4-x}\mathrm{Fe}^{3+}_x)^6(\mathrm{Al})_2\mathrm{O}_{10}(\mathrm{OH})_2M^+_x$ is theoretical.

EXTENT OF OCTAHEDRAL SUBSTITUTIONS

$^6(\mathrm{Mg} - \mathrm{Fe}^{3+})$

Grauby *et al.* (1994) showed that a continuous octahedral solid solution exists between the ferric nontronite ($^4(\mathrm{Si}_{4-x}\mathrm{Fe}^{3+}_x)^6\mathrm{Fe}^{3+}_2\mathrm{O}_{10}(\mathrm{OH})_2M^+_x$) and ferric

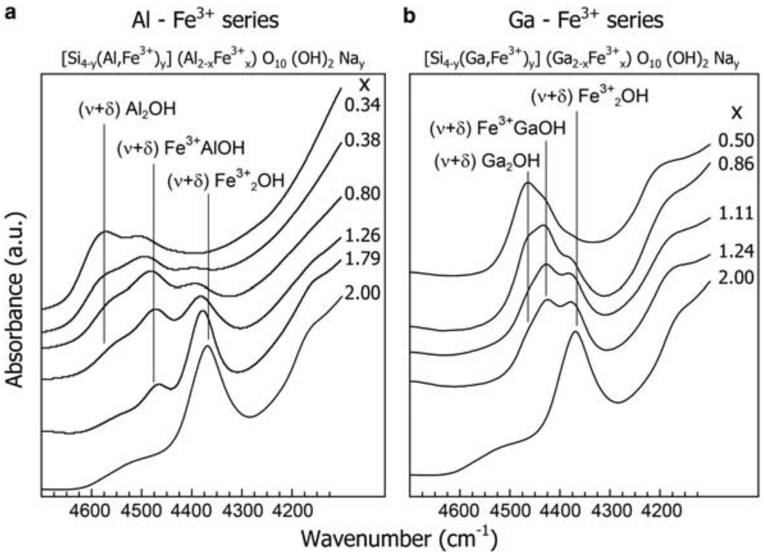

FIG. 4. NIR spectra in the OH combination bands region of (a): Al-Fe^{3+} nontronites (selected from Petit *et al.*, 2015); (b): Ga-Fe^{3+} nontronites (selected from Petit *et al.*, 2016).

saponite ($(^4(Si_{4-x}Fe^{3+}{}_x)^6(Mg_3)O_{10}(OH)_2M^+{}_x)$ end-members, with no chemical gap, unlike that which was suggested by Weaver & Pollard (1973) from the chemistry of natural smectites. This solid solution series implies a mixing of local di- and trioctahedral sites occupancies forming small domains within layers which were revealed accordingly by FTIR spectroscopy through OH-stretching bands due to the occurrence of Mg and Fe^{3+} neighbouring octahedral cations (see above).

$$^6(Mg - (Fe^{3+} + Fe^{2+}))$$

Baldermann *et al.* (2014) proposed the possibility of a complete octahedral substitution rate between Mg and ($Fe^{3+} + Fe^{2+}$) in saponites. The Mg- and Fe-richest saponite end-members synthesized by Baldermann *et al.* (2014) had ($Mg_{2.3}Fe^{2+}_{0.42}Fe^{3+}_{0.04}$) and ($Mg_{0.26}Fe^{2+}_{2.26}Fe^{3+}_{0.21}$) octahedral compositions, respectively.

$$^6(Fe^{2+} - Fe^{3+})$$

Although many syntheses of Fe smectites were performed under partly reducing conditions, the occurrence of some octahedral Fe^{2+}, generally measured using Mössbauer spectroscopy, has rarely been reported (Mizutani *et al.*, 1991; Lajarige *et al.*, 1998). The composition of the octahedral sheet was reported by Mizutani *et al.* (1991) to be $^6(Fe^{3+}_{1.9}Fe^{2+}_{0.1})$ and by Lajarige *et al.* (1998) to be $^6(Al_{1.06}Fe^{3+}_{0.8}Fe^{2+}_{0.2})$. Only a small $^6Fe^{2+}$–$^6Fe^{3+}$ range was then explored experimentally, probably because it is difficult to prevent the oxidation of Fe during experiments or even after syntheses (Baldermann *et al.*, 2014).

$$^6(M^{3+} - Fe^{3+})$$

In the ternary Fe^{3+}/Al/Mg diagram of Güven (1988), a large chemical gap between beidellite and nontronite was suggested for natural dioctahedral smectites. These natural dioctahedral smectites very often contain Mg (Gates, 2005) and the octahedral Al-Fe^{3+} solid solution is complete only as long as Mg is present in the system (Gaudin *et al.*, 2004a,b). Andrieux & Petit (2010) and Petit *et al.* (2015) showed that a complete Al-Fe^{3+} octahedral solid solution does exist along the join Al (beidellite)–Fe^{3+} (nontronite) $[^4(Si_{4-x}(Al\text{-}Fe^{3+})_x)^6(Al\text{-}Fe^{3+})_2O_{10}(OH)_2M^+{}_x]$, with no Mg. Similarly, Ga^{3+} can substitute easily for Fe^{3+} in the octahedral sheet of dioctahedral smectites forming a complete solid solution (Petit *et al.*, 2016). Moreover, for these two binary Al-Fe^{3+} and Ga-Fe^{3+} smectitic solid solutions, combination bands in IR spectra (Fig. 4) revealed that octahedral cations are always distributed randomly (see Petit *et al.* (2015) and Petit *et al.* (2016), for Al-Fe^{3+} and Ga-Fe^{3+}, respectively).

KINETICS OF Fe-SMECTITE SYNTHESIS

Nontronites and Fe^{3+}-beidellites were synthesized over a wide range of temperatures ($3 < T < 350$°C), generally within few days (Table 1). For a given synthesis time, an increase in synthesis temperature leads to an increase in the crystal order of the smectites (Decarreau *et al.*, 2008). The transformation rate of starting materials (mainly co-precipitated gels) is time- and temperature-dependent and, for low-temperature syntheses, amorphous and/or unreacted products were observed for short synthesis times (Harder, 1976, 1978; Farmer *et al.*, 1991).

Many syntheses used starting gels containing Fe^{2+} or Mg cations, partly on the basis of previous results showing that it was easy to synthesize trioctahedral M^{2+}-smectites (Strese & Hofmann, 1941). But syntheses of Fe smectites were also performed successfully under strictly oxidizing conditions and without Mg (Table 1). Nevertheless the kinetics of synthesis seems to be greater when the starting gel contains Fe^{2+}: a relatively well crystallized ferric nontronite was synthesized at 75°C over 15 days from a ferrous gel (Decarreau *et al.*, 1986) while with a ferric gel, at the same temperature, only the beginning of crystallization of a ferric nontronite was observed after 1 month of synthesis (Decarreau *et al.*, 1987). However, the pH was not the same and the two experiments were not directly comparable.

When ferrous starting gels were used, generally, smectites synthesized in oxidizing conditions contained only ferric iron (Table 1). Under partial anaerobic conditions, Fe^{2+} cations might remain in synthesized smectites and the oxidation process is rather slow (Mizutani *et al.*, 1991; Lajarige *et al.*, 1998). These results suggest that the occurrence of Fe^{2+} in natural smectites does not necessary result from a long exposure time under reducing conditions.

METASTABILITY OF Na-FERRIC NONTRONITE

In the Si, Fe^{3+}, Na, H_2O system, three silicate minerals may form: ferripyrophyllite, ferric nontronite and aegirine. True ferripyrophyllite has never been synthesized (Lantenois *et al.*, 2007), while Grauby (1993) synthesized a 2:1 ferric silicate similar to ferripyrophyllite (that author synthesized a non-swelling layered Si-Fe^{3+} mineral with a 9–10 Å XRD reflection). Aegirine is a common by-product of nontronite syntheses (Kopp, 1967; Nagase *et al.*, 1999; Baron, 2016). Baron (2016) studied the evolution at 150°C of a starting gel with a $Si_2FeNa_2O_6$ composition at pH 12 and 13.3 from 1–183 days. For experiments at pH 13.3, during the first 15 days, a high-charge ferric nontronite was synthesized which disappeared progressively and was replaced by the aegirine + hematite paragenesis in long-time syntheses. In this chemical system, nontronite appears as a metastable phase, kinetically favoured, aegirine being the true stable silicate phase. In the Si, Fe^{3+}, K, H_2O system, the ferric mica appeared as the stable silicate phase, probably because the potassic equivalent to aegirine does not exist (Baron, 2016). The calcic equivalent to aegirine does not exist either. Farmer *et al.* (1994) and Tomita *et al.* (1993) observed dotted electron diffraction patterns characteristic of a 3D stacking for Fe-rich smectites synthesized with Ca available in solution: $Ca(OH)_2$ was used as a pH buffer by Farmer *et al.* (1994) and Ca coming from the dissolution of the starting volcanic glass by Tomita *et al.* (1993). Similar syntheses performed with NaOH or KOH by Farmer *et al.* (1994) produced Fe-smectite particles giving electron diffraction patterns with continuous rings typical of turbostratic stacking layers as commonly observed for other synthesized smectites and for smectite in general. Unfortunately, not enough data are available, notably concerning syntheses with long duration times, to be able to evaluate the comparative ‘stability’ of the Fe-smectite synthesized *vs.* the interlayer cation.

CONCLUSIONS

Eight decades of synthesis of nontronite and other Fe-rich smectites have shown that smectite can form at rather low temperatures, typically from ambient to 200°C, under various redox conditions, from either Fe^{2+} or Fe^{3+} starting gels. The purity of the sample and the structural Fe^{3+} content in the smectite is controlled by pH and temperature conditions. The octahedral homovalent Al^{3+}-Fe^{3+} substitution in smectites is complete and continuous, while the tetrahedral Fe^{3+} content depends on the Al^{3+}/Fe^{3+} ratio of the smectite. Many experimental investigations are still needed to explore and fine-tune the Fe^{2+}-Fe^{3+} octahedral solid solution in smectite as well as to study the possible role of organic matter in smectite crystallization and in the crystal chemistry of the smectite formed.

This review has provided evidence of the crucial importance of detailed characterization of the samples synthesized. Very often, the use of multiple analytical techniques is required. Among them, both XRD and IR spectroscopy are required at least to characterize samples in a known chemical system. Mössbauer spectroscopy is appropriate for detecting and quantifying the amounts of Fe^{2+}, but not of tetrahedral Fe^{3+}, in smectites. XANES offers promise as a means of measuring tetrahedral Fe^{3+} (Decarreau *et al.*, 2008) and deserves to be evaluated with chemical series of synthetic nontronites with various known $^{4}Fe^{3+}$, such as the chemical series of Baron *et al.* (2016a) described above.

REFERENCES

Andrieux P. & Petit S. (2010) Hydrothermal synthesis of dioctahedral smectites: The Al-Fe chemical series. Part I: Influence of experimental conditions. *Applied Clay Science*, **48**, 5–17.

Baldermann A., Dohrmann R., Kaufhold S., Nickel C., Leetofsky-Papst I. & Dietzel M. (2014) The Fe-Mg-saponite solid solution series: a hydrothermal synthesis study. *Clay Minerals*, **49**, 391–415.

Baron F. (2016) *Le fer dans les smectites: une approche par synthèse minérale*. PhD thesis, Poitiers University, France.

Baron F., Petit S., Tertre E. & Decarreau A. (2016a) Influence of aqueous Si and Fe speciation on tetrahedral Fe(III) substitutions in nontronites: A clay synthesis approach. *Clays and Clay Minerals*, **64**, 189–203.

Baron F., Pushparaj S.S.C., Fontaine C., Sivaiah M.V., Decarreau A. & Petit S. (2016b) Microwave-assisted hydrothermal synthesis of Ni-Mg layered silicate clays. *Current Microwave Chemistry*, **3**, 85–89.

Baron F., Petit S., Pentrák M., Decarreau A. & Stucki J. (2017) Revisiting the nontronite Mössbauer spectra. *American Mineralogist*, **102**, 1501–1515.

Berger G., Meunier A. & Beaufort D. (2014) Clay mineral formation on Mars: Chemical constraints and possible contribution of basalt out-gassing. *Planetary and Space Science*, **95**, 25–32.

Bonnin, D., Calas, G., Suquet, H., & Pezerat, H. (1985) Sites occupancy of Fe^{3+} in Garfield nontronite: A spectroscopic study. *Physics and Chemistry of Minerals*, **12**, 55–64.

Brigatti M.F., Galán E. & Theng B.K.G. (2013) Structure and mineralogy of clay minerals. Smectites. Pp. 42–45 in: *Handbook of Clay Sciences*, 2nd edition (F. Bergaya & G. Lagaly, editors). Elsevier, Amsterdam.

Caillère S., Hénin S. & Esquevin J. (1953) Synthèses à basse température de phyllites ferrifères. *Comptes Rendus Académie Sciences (Paris)*, **237**, 1724–1726.

Caillère S., Hénin S. & Esquevin J. (1955) Synthèses à basse température de quelques minéraux ferrifères (silicates, oxydes). *Bulletin Société Française Minéralogie Cristallographie*, **78**, 227–241.

Cardile C.M. & Johnston J.H. (1985) Structural studies of nontronites with different iron contents by ^{57}Fe Mössbauer spectroscopy. *Clays and Clay Minerals*, **33**, 295–300.

Carter J., Poulet F., Bibring J.-P., Mangold N. & Murchie S. (2013) Hydrous minerals on Mars as seen by the CRISM and OMEGA imaging spectrometers: Updated global view. *Journal of Geophysical Research: Planets*, **118**, 831–858.

Carter J., Loizeau D., Mangold N., Poulet F. & Bibring J.-P. (2015) Widespread surface weathering on early Mars: A case for a warmer and wetter climate. *Icarus*, **248**, 373–382.

Cashion J.D., Gates W.P. & Thomson A. (2008) Mössbauer and IR analysis of iron sites in four ferruginous smectites. *Clay Minerals*, **43**, 83–93.

Decarreau A. & Bonnin D. (1986) Synthesis and crystallogenesis at low temperature of Fe (III)-smectites by evolution of coprecipitated gels: Experiments in partially reducing conditions. *Clay Minerals*, **21**, 861–877.

Decarreau A. & Petit S. (2014) Fe^{3+}/Al^{3+} partitioning between tetrahedral and octahedral sites in dioctahedral smectites. *Clay Minerals*, **49**, 657–665.

Decarreau A., Bonnin D., Badaut-Trauth D., Couty R. & Kaiser P. (1987) Synthesis and crystallogenesis of ferric smectite by evolution of Si-Fe coprecipitates in oxidizing conditions. *Clay Minerals*, **22**, 207–223.

Decarreau A., Petit S., Vieillard Ph. & Dabert N. (2004) Hydrothermal synthesis of aegirine at 200°C. *European Journal of Mineralogy*, **16**, 85–90.

Decarreau A., Petit S., Martin F., Farges F., Vieillard P. & Joussein E. (2008) Hydrothermal synthesis, between 75 and 150°C, of high charge ferric nontronites. *Clays and Clay Minerals*, **56**, 322–337.

Ehlmann B.L., Berger G., Mangold N., Michalski J.R., Catling D.C., Ruff S.W., Chassefière E., Niles P.B., Chevrier V. & Poulet F. (2013) Geochemical consequences of widespread clay mineral formation in Mars' ancient crust. *Space Science Reviews*, **174**, 329–364.

Ewell R.H. & Insley H. (1935) Hydrothermal synthesis of kaolinite, dickite, beidellite and nontronite. *Journal of the National Bureau of Standards*, **15**, 173–186.

Farmer V.C. (1997) Conversion of ferruginous allophones to ferruginous beidellites at 95°C under alkaline conditions with alternating oxidation and reduction. *Clay and Clay Minerals*, **45**, 591–597.

Farmer V.C., Krishnamurti G.S.R. & Huang P.M. (1991) Synthetic allophone and layer-silicates formation in SiO_2-Al_2O_3-FeO-Fe_2O_3-MgO-H_2O systems at 23°C and 89°C in a calcareous environment. *Clays and Clay Minerals*, **39**, 561–570.

Farmer V.C., McHardy W.J., Elsass F. & Robert M. (1994) *hk*-ordering in aluminous nontronite and saponite synthesized near 90°C: effects of synthesis conditions on nontronite composition and ordering. *Clays and Clay Minerals*, **42**, 180–186.

Gates W.P. (2005) Infrared spectroscopy and the chemistry of dioctahedral smectites. Pp. 125–168 in: *The Application of Vibrational Spectroscopy to Clay Minerals and Layered Double Hydroxides* (J.T.

Kloprogge, editor). CMS Workshop Lectures, **13**, The Clay Minerals Society, Aurora, Colorado, USA.

Gaudin A., Grauby O., Noack Y., Decarreau A. & Petit S. (2004a) The actual crystal chemistry of ferric smectites from the lateritic nickel ore of Murin Murin (Western Australia). I. XRD and multi-scale chemical approaches. *Clay Minerals*, **39**, 301–315.

Gaudin A., Petit S., Rose J., Martin F., Decarreau A., Noack Y. & Borscheneck D. (2004b) The accurate crystal chemistry of ferric smectites from the lateritic nickel ore of Murrin Murrin (Western Australia). II. Spectroscopic (IR and EXAFS) approaches. *Clay Minerals*, **39**, 453–467.

Goodman B.A, Russell J.D, Fraser A.D & Woodhams F. W.D (1976) A Mössbauer and IR spectroscopic study of the structure of nontronite. *Clays Clay Minerals*, **24**, 53–59.

Grauby O. (1993) *Nature et étendue des solutions solides octaèdriques argileuses. Approche par synthèse minérale*. PhD thesis, Poitiers University, France

Grauby O., Petit S., Decarreau A. & Baronnet A. (1994) The nontronite–saponite series: an experimental approach. *European Journal of Mineralogy*, **6**, 99–112.

Gupta V.K, Mohan D. & Saini V.K (2006) Studies on the interaction of some azo dyes (naphthol red-J and direct orange) with nontronite mineral. *Journal of Colloid and Interface Science*, **298**, 79–86.

Güven N. (1988) Smectites. Pp. 497–559 in: *Hydrous Phyllosilicates (Exclusive of Micas)*. (S.W. Bailey, editor). Reviews in Mineralogy, **19**. Mineralogical Society of America, Washington, D.C.

Hamilton G. & Furtwängler W. (1951) Synthese von Nontronit. *Tschermaks Mineralogishe und Petrographische Mitteilungen*, **2**, 397–406.

Harder H. (1976) Nontronite synthesis at low temperature. *Chemical Geology*, **18**, 169–180.

Harder H. (1978) Synthesis of iron layer silicate minerals under natural conditions. *Clays and Clay Minerals*, **26**, 65–72.

Hofstetter T.B, Neumann A. & Schwarzenbach R.P (2006) Reduction of nitroaromatic compounds by Fe (II) species associated with iron-rich smectites. *Environmental Science & Technology*, **40**, 235–242.

Ilgen A.G, Foster A.L & Trainor T.P (2012) Role of structural Fe in nontronite NAu-1 and dissolved Fe(II) in redox transformations of arsenic and antimony. *Geochimica et Cosmochimica Acta*, **94**, 128–145.

Jaisi D.P, Dong H., Plymale A.E, Fredrickson J.K, Zachara J.M, Heald S. & Liu C.(2009) Reduction and long-term immobilization of technetium by Fe(II) associated with clay mineral nontronite. *Chemical Geology*, **264**, 127–138.

Kaufhold S., Stucki J.W., Finck N., Steininger R., Zimina A., Dohrmann R., Ufer K., Pentrák M. & Pentráková L. (2017) Tetrahedral charge and Fe content in dioctahedral smectites. *Clay Minerals*, **52**, 51–65.

Kloprogge J.T., Komarneni S. & Amonette E. (1999) Synthesis of smectite clay minerals: a critical review. *Clays and Clay Minerals*, **47**, 529–554.

Kopp O.C. (1967) Synthesis of grunerite and other phases in the system SiO_2-NaOH-Fe-H_2O. *American Mineralogist*, **52**, 1681–1688.

Lajarige C., Petit S., Augas C. & Decarreau A. (1998) Stabilisation of Fe^{2+} ions in synthetic ferroan smectites. *Comptes Rendus Académie Sciences Paris*, **327**, 789–794.

Lantenois S., Beny J.M., Muller F. & Champellier R. (2007) Integration of Fe in natural and synthetic Al-pyrophyllites: an infrared spectroscopic study. *Clays and Clay Minerals*, **42**, 129–141.

Li H., Li Y., Xiang L., Huang Q., Qiu J., Zhang H., Sivaiah M.V., Baron F., Barrault J., Petit S. & Valange, S. (2015) Heterogeneous photo-Fenton decolorization of Orange II over Al-pillared Fe-smectite: Response surface approach, degradation pathway, and toxicity evaluation. *Journal of Hazardous Materials*, **287**, 32–41.

Liu R., Xiao D., Guo Y., Wang Z. & Liu, J. (2014) A novel photosensitized Fenton reaction catalyzed by sandwiched iron in synthetic nontronite. *RSC Advances*, **4**, 12958–12963.

MacGregor-Ramiasa M., Abrahamsson C., Röding M. & Nydén M. (2015) Magnetic alignment of nontronite dispersions. *Applied Clay Science*, **116**, 167–174.

Madejová J., Komadel P. & Čičel B. (1994) Infrared study of octahedral site populations in smectites. *Clay Minerals*, **29**, 319–326.

Mangold N., Baratoux D., Witasse O., Encrenaz T. & Sotin C. (2016) Mars: a small terrestrial planet. *The Astronomy and Astrophysics Review*, **24**, 15.

Meunier A., Mas A., Beaufort D., Patrier P. & Dudoignon P. (2008) Clay minerals in basalt-hawaiite rocks from Mururoa atoll, French Polynesia. II. Petrography and geochemistry. *Clays and Clay Minerals*, **56**, 730–750.

Meunier A., Petit S., Ehlmann B.L., Dudoignon P., Westall F., Mas A., El Albani A. & Ferrage E. (2012) Magmatic precipitation as a possible origin of Noachian clays on Mars. *Nature Geoscience*, **5**, 739–743.

Michot L.J., Bihannic I., Maddi S., Baravian C., Levitz P. & Davidson P. (2008) Sol-gel and isotropic/nematic transitions in aqueous suspensions of natural nontronite clay. Influence of particle anisotropy. 1. features of the I.N transition. *Langmuir*, **24**, 3127–3139.

Michot L.J, Baravian C., Bihannic I., Maddi S., Moyne C., Duval J.F.L., Levitz P. & Davidson P. (2009) Sol-gel and isotropic/nematic transitions in aqueous suspensions of natural nontronite clay. Influence of particle anisotropy. 2. Gel structure and mechanical properties. *Langmuir*, **25**, 127–139.

Michot L.J., Paineau E., Bihannic I., Maddi S., Duval J.F.L., Baravian C., Davidson P. & Levitz P. (2013) Isotropic/nematic and sol/gel transitions in aqueous suspensions of size selected nontronite NAu-1. *Clay Minerals*, **48**, 663–685.

Milliken R.E., & Bish D.L. (2010) Sources and sinks of clay minerals on Mars. *Philosophical Magazine*, **90**, 2293–2308.

Mizutani T., Fukushima Y., Okada A., Kamigaito O. & Kobayashi T (1991) Synthesis of 1:1 and 2:1 iron phyllosilicates and characterization of their iron state by Mössbauer spectroscopy. *Clay and Clay Minerals*, **39**, 381–386.

Mustard J.F., Murchie S.L., Pelkey S.M., Ehlmann B.L., Milliken R.E., Grant J.A., Bibring J.-P., Poulet F., Bishop J., Dobrea E.N. *et al.* (2008) Hydrated silicate minerals on Mars observed by the Mars Reconnaissance Orbiter CRISM instrument. *Nature*, **454**, 305–309.

Nagase T., Iwasaki T., Ebina T., Hayashi H., Onodera Y. & Chandra Dutta N. (1999) Hydrothermal synthesis of Fe-montmorillonite in Si-Fe-Mg system. *Chemistry Letters*, **4**, 303–304.

Neumann A., Hofstetter T.B., Skarpeli-Liati M. & Schwarzenbach R.P (2009) Reduction of polychlorinated ethanes and carbon tetrachloride by structural Fe(II) in smectites. *Environmental Science & Technology*, **43**, 4082–4089.

Oyawoye M.O. & Hirst D.M. (1964) Occurrence of a montmorillonite mineral in the Nigerian younger granites at Ropp, Plateau Province, northern Nigeria. *Clay Minerals*, **5**, 427–433.

Paineau E., Philippe A.M., Antonova K., Bihannic I., Davidson P., Dozov I., Gabriel J.C.P., Impéror-Clerc M., Levitz P., Meneau F. & Michot L.J. (2013) Liquid–crystalline properties of aqueous suspensions of natural clay nanosheets. *Liquid Crystals Reviews*, **1**, 110–126.

Petit S., Decarreau A., Gates W., Andrieux P. & Grauby O. (2015) Hydrothermal synthesis of dioctahedral smectites: The Al–Fe^{3+} chemical series. Part II: Crystal chemistry. *Applied Clay Science*, **104**, 96–105.

Petit S., Baron F., Grauby O. & Decarreau A. (2016) Revisiting the cation mass-valence sum approach to assigning infrared OH-bands in dioctahedral smectites in the light of new data from synthetic Ga-Fe^{3+} smectites. *Vibrational Spectroscopy*, **87**, 137–142.

Poulet F., Bibring J.P., Mustard J.F., Gendrin A., Mangold N., Langevin Y., Arvidson R.E., Gondet B., Gomez C. & the Omega team (2005) Phyllosilicates on Mars and implications for early Martian climate. *Nature*, **438**, 623–637.

Slonimskaya M.V., Besson G., Daynyak L.G., Tchoubar C. & Drits V.A. (1986) Interpretation of the IR spectra of celadonites, glauconites in the region of OH-stretching frequencies. *Clay Minerals*, **21**, 377–388.

Strese H. & Hofmann U. (1941) Synthesis of magnesian silicate gels with two dimensional regular structure. *Zeitschrift für Anorganishe und Allgemeine Chemie*, **247**, 65–95.

Tomita K., Yamane H. & Kawano M. (1993) Synthesis of smectite from volcanic glass at low temperature. *Clays and Clay Minerals*, **41**, 655–661.

Weaver C.E. & Pollard L.D. (1973) *The Chemistry of Clay Minerals*. Elsevier, London.

Wilson M.J. (2013) Smectite clay minerals (beidellite, pp. 257–277; nontronite, pp. 278–299) in: *Sheet Silicates, Rock-Forming Minerals*, **vol. 3C** (W.A. Deer, R.A. Howie & J. Zussman, editors). The Geological Society, London.

Wray J.J., Murchie S.L., Squyres S.W., Seelos F.P. & Tornabene L.L. (2009) Diverse aqueous environments on ancient Mars revealed in the southern highlands. *Geology*, **37**, 1043–1046.

Yang J., Kukkadapu R.K., Dong H., Shelobolina E.S., Zhang J. & Kim J. (2012) Effects of redox cycling of iron in nontronite on reduction of technetium. *Chemical Geology*, **291**, 206–216.

Zen J.-M., Jeng S.-H. & Chen, H.-J. (1996) Catalysis of the electroreduction of hydrogen peroxide by nontronite clay coatings on glassy carbon electrodes. *Journal of Electroanalytical Chemistry*, **408**, 157–163.

Zhang D., Zhou C.-H., Lin C.-X., Tong D.-S. & Yu W.-H. (2010) Synthesis of clay minerals. *Applied Clay Science*, **50**, 1–11.

Zhou C-H. (2010) Emerging trends and challenges in synthetic clay-based materials and layered double hydroxides. *Applied Clay Science*, **48**, 1–4.